

Magnetic Transition Temperature of (La,Sr)MnO₃

Nobuo FURUKAWA

*Institute for Solid State Physics,
University of Tokyo, Roppongi 7-22-1,
Minato-ku, Tokyo 106*

Abstract

Using the Kondo lattice model with classical spins in infinite dimension, magnetic phase transition in the perovskite-type 3d transition-metal oxide $\text{La}_{1-x}\text{Sr}_x\text{MnO}_3$ is theoretically studied. On the Bethe lattice, the self-consistency equations are solved exactly. Curie temperatures at the region of double-exchange ferromagnetism $0.1 \lesssim x \lesssim 0.25$ as well as the Nèel temperature at $x = 0$ are well reproduced quantitatively. Pressure effect on the Curie temperature is also discussed.

KEYWORDS: Transition-metal oxide, manganese oxide, double-exchange ferromagnetism, Kondo lattice model, infinite dimensions

After the discovery of high T_c oxides, the physics of strongly correlated $3d$ transition-metal oxide compounds have been revisited extensively. One of such materials is the perovskite-type manganese oxides $\text{La}_{1-x}\text{Sr}_x\text{MnO}_3$. The most prominent feature of the system is the giant magnetoresistance (GMR) with negative sign. The system is a double-exchange ferromagnet^{1,2)} at $x \gtrsim 0.1$, while the antiferromagnetic phase with spin canting is observed at $x \sim 0$. For the detail of the phase diagram and the GMR in $\text{La}_{1-x}\text{Sr}_x\text{MnO}_3$ and related materials, the readers are referred to *e.g.* refs. 3 and 4, and those cited therein.

In $\text{La}_{1-x}\text{Sr}_x\text{MnO}_3$, $3d$ electrons are considered to form both localized spins with $S = 3/2$ in the t_{2g} orbitals and itinerant electrons in the e_g orbitals which are coupled each other by Hund's ferromagnetic interaction. The bandwidth of the itinerant electron is estimated to be $W \sim 1\text{eV}$ from the recent band calculation,⁵⁾ while the Hund's coupling is considered to be larger than the bandwidth. As a model Hamiltonian of this system, the Kondo lattice model (KLM) with $S = 3/2$ and the ferromagnetic exchange coupling has been proposed.⁶⁾

From the strong coupling limit of the above model, Curie temperature T_c has been studied.^{2,6)} Using a mean-field type treatment, Curie temperature is estimated to be $T_c \sim W$, where W is the bandwidth of the conduction electron. This result is roughly understood as follows; the transition temperature is determined from the competition between the gain of kinetic energy in the ferromagnetic state and the gain of entropy in the paramagnetic state.

Quantitatively, however, the mean-field approach fails to explain the experimental value of T_c , *e.g.* $T_c \sim 300\text{K}$ at $x \sim 0.2$ which is a few orders of magnitude lower than the theoretical estimate. The discrepancy seems to be due to the fact that the mean-field treatment poorly describes the electronic state in the paramagnetic phase so that kinetic energy is not estimated properly. In the paramagnetic phase, thermal spin fluctuations have to be taken into account appropriately because the system is in a strongly correlated regime. Recently, Millis *et.al.* has made an analysis on T_c based on the calculation of the spin stiffness at the ground state.⁷⁾ Their result also overestimates T_c . Since the changes in the electronic state from the ferromagnetic ground state to the paramagnetic state should be nontrivial and drastic, ground state properties may not reproduce the transition temperature. Because the GMR is most prominently observed in the vicinity of the Curie temperature, a theoretical approach which is able to predict T_c with accuracy is demanded also from the standpoint of a material designing and applications.

The author has shown in his previous work^{3,8,9)} that the KLM in infinite dimensional limit $D = \infty$ and infinite high-spin limit $S = \infty$ reproduces the transport properties of $\text{La}_{1-x}\text{Sr}_x\text{MnO}_3$ quantitatively. Within these limits, Green's functions are obtained exactly even in the paramagnetic state. Therefore, a proper treatment is possibly performed to obtain magnetic instabilities in the paramagnetic phase. In this paper, we study the magnetic phase transition of the above model. One of the aims is to examine, within this model, whether it is possible to explain the magnitude of the Curie temperature as well as its doping dependence in a consistent way.

Thus we investigate the KLM at $D = \infty$ and $S = \infty$. The Hamiltonian is described as

$$\mathcal{H} = -t \sum_{\langle ij \rangle, \sigma} (c_{i\sigma}^\dagger c_{j\sigma} + h.c.) - J \sum_i \vec{\sigma}_i \cdot \vec{m}_i, \quad (1)$$

where $\vec{m}_i = (m_i^x, m_i^y, m_i^z)$ and $|\vec{m}|^2 = 1$. We consider the Bethe lattice in the infinite coordination number limit. From the nature of the Bethe lattice that lattice points are divided into two sublattices, it is possible to study magnetic phases with ferromagnetic and antiferromagnetic order parameters. The density of states (DOS) is given in the semi-circular form $N_0(\varepsilon) = (2/\pi W) \sqrt{1 - (\varepsilon/W)^2}$, where W is the bandwidth. Here we see another advantage of the Bethe lattice that the DOS has similar properties to that of the $D = 3$ systems, namely the existence of a band edge and the shape of the DOS at the edge. The above properties may be important in the case of making comparisons between the theoretical results and the experimental data in the low hole concentration region.

The infinite-dimensional model is mapped to that of the corresponding single-cell model. The partition function is written in a form

$$Z = \iint d\Omega_A d\Omega_B Z_f(\vec{m}_A, \vec{m}_B), \quad (2)$$

where integration is performed with respect to the orientation of local spins. Using the Weiss fields $\tilde{G}_{0\alpha}(i\omega_n)$ which describe the dynamical motions of electrons for $\alpha = A, B$ sublattice sites, the fermion trace is given by

$$Z_f(\vec{m}_A, \vec{m}_B) = \prod_{\alpha=A,B} 4 \exp \left(\sum_n \log \det \left[\frac{(\tilde{G}_{0\alpha}^{-1} + J\vec{m}_\alpha \vec{\sigma})}{i\omega_n} \right] e^{i\omega_n 0_+} \right). \quad (3)$$

The Green's function is calculated exactly as

$$\tilde{G}_\alpha(i\omega_n) = \iint d\Omega_A d\Omega_B \frac{Z_f(\vec{m}_A, \vec{m}_B)}{Z} \left(\tilde{G}_{0\alpha}^{-1}(i\omega_n) + J\vec{m}_\alpha \vec{\sigma} \right)^{-1}. \quad (4)$$

On the Bethe lattice with two-sublattice symmetry, the mapping relation gives¹⁰⁾

$$\begin{aligned} \tilde{G}_{0A}^{-1}(i\omega_n) &= i\omega_n + \mu - \tilde{G}_B(i\omega_n)/4, \\ \tilde{G}_{0B}^{-1}(i\omega_n) &= i\omega_n + \mu - \tilde{G}_A(i\omega_n)/4. \end{aligned} \quad (5)$$

Self-consistency equations (2)-(5) are mainly solved in a numerical way. At $J/W \gg 1$, Green's functions near the magnetic transition temperature are also studied analytically.

Sublattice magnetization of the local spins $\langle \vec{m}_\alpha \rangle$ is obtained from

$$\langle \vec{m}_\alpha \rangle = \iint d\Omega_A d\Omega_B \vec{m}_\alpha \frac{Z_f(\vec{m}_A, \vec{m}_B)}{Z}. \quad (6)$$

Then, magnetic transition temperatures are determined as a function of Hund's coupling J and chemical potential μ in the unit of W . The carrier electron number for $\text{La}_{1-x}\text{Sr}_x\text{MnO}_3$ is nominally considered to be $n = 1 - x$. Hereafter we use the hole picture so that the hole concentration is expressed by $\langle x \rangle = 1 - \langle n \rangle$. In this paper, we restrict ourselves to $0 \leq \langle x \rangle \lesssim 0.5$, *i.e.* from half-filling to quarter-filling.

In Fig. 1, we show T_c/W as a function of J/W at various filling. Here, for simplicity of the calculation, chemical potentials are systematically chosen to be $\mu(J) = -J + \delta\mu$ with $\delta\mu/W = 0, 0.25$ and 0.33 so that the carrier numbers at T_c become $\langle x \rangle \simeq 0.5, 0.3$ and 0.2 , respectively, with errors $\lesssim \pm 0.03$ at $J/W \geq 4$. The curves in the figure are the results of the $(J/W)^{-1}$ expansion at $J/W \gg 1$ in the form

$$T_c/W = \tilde{T} \left[1 - \tilde{J}(J/W)^{-1} \right]. \quad (7)$$

We see $T_c \propto W$ at $J/W \rightarrow \infty$. Dimensionless constants are given by $\tilde{T} \simeq 0.044, 0.039$ and 0.035 while $\tilde{J} \simeq 0.49, 0.89$ and 1.12 for $\langle x \rangle \sim 0.5, 0.3$ and 0.2 , respectively. The fitting curves seems to reproduce results also at $J/W \sim 1$ surprisingly well. The quantity \tilde{T} is the Curie temperature in the scale of W at $J/W \rightarrow \infty$, while \tilde{J} may be interpreted as the magnitude of the instability of the ferromagnetic order upon decrease of J/W . From $\tilde{T} \sim 0.04$ and $W \sim 10^4\text{K}$, we see that the Curie temperature in $\text{La}_{1-x}\text{Sr}_x\text{MnO}_3$ is roughly explained within this model in the strong coupling limit. The tendency that \tilde{T}

(\tilde{J}) increases (decreases) as holes are doped is easily understood because the stability of the ferromagnetic order should be enhanced by hole doping.

Now, we precisely compare the doping dependence of T_c with the experimental data. Calculations are performed at $J/W = 4$ which is the value that explains the magnetoresistance phenomena successfully,³⁾ as well as at $J/W = \infty$. In Fig. 2, we show T_c as a function of x together with the experimental data from ref. 4. Here, the bandwidth is scaled so that T_c at $x = 0.15$ reproduces the experimental result; we then have $W = 1.05\text{eV}$ for $J/W = 4$, which is a moderate value. Thus we see from the above result that the experimental data are quantitatively reproduced very well at $x \lesssim 0.25$. Discrepancy on the doping dependence of T_c is observed at $x \gtrsim 0.3$, which may be interpreted as a sign of a crossover of the system from the strong coupling regime to a weak coupling limit.

Next, we calculate the pressure effect on T_c . In $\text{La}_{1-x}\text{Sr}_x\text{MnO}_3$ at the ferromagnetic metal region $x \gtrsim 0.15$, increase of T_c is observed under pressure.¹¹⁾ The pressure coefficient $d \log T_c / dP$ is positive, and it decreases systematically as the hole concentration is increased. For the theoretical treatment, we make following assumptions; the bandwidth increases as pressure is applied due to the increase of overlaps between neighboring orbitals, while the intra-atomic Hund's coupling is not affected. Then, we have

$$\frac{d \log T_c}{dP} = \frac{d \log W}{dP} \frac{\partial \log T_c}{\partial \log W}, \quad (8)$$

where $d \log W / dP > 0$ from the assumption. Using eq. (7) at $J \gg \tilde{J}W$, we have

$$\frac{\partial \log T_c}{\partial \log W} \simeq 1 - \tilde{J}(J/W)^{-1}, \quad (9)$$

so that a positive pressure coefficient is derived in the strong coupling region. We have shown above that \tilde{J} decreases as x is increased. Then, the pressure coefficient of T_c should increase by hole doping if J/W is fixed, which is contrary to the experimental result. In order to explain the experiment within the present model and the assumptions mentioned above, we must have the effective decrease in J/W as the hole concentration is increased. This is another implication that the system undergoes the crossover to the weak coupling region by hole doping.

In Fig. 3, the Nèel temperature T_N at $x = 0$ is shown. At $J \gg W$, the expansion with respect to $(J/W)^{-1}$ gives an analytical formula

$$T_N/W = (1/24) \cdot (J/W)^{-1}. \quad (10)$$

The Néel temperature in LaMnO_3 , $T_N \simeq 140\text{K}$,⁴⁾ is also well explained, *e.g.* if we set $J = 4W$ and $W \simeq 1.2\text{eV}$. Upon hole doping, the model in the low temperature regime shows a first order transition from the Néel state directly to the ferromagnetic state. Canted Néel state which is observed in $\text{La}_{1-x}\text{Sr}_x\text{MnO}_3$ at $x \lesssim 0.1$ is not found within this model at $J/W \gtrsim 2$. It must be noted that the present approach does not take into account the magnetic phase with incommensurate wave numbers such as spiral states or conical states. In order to study the magnetic structure at $x \lesssim 0.1$, it seems to be necessary to treat the model in a realistic lattice structure. Effects from the orbital degeneracy in e_g bands and its Jahn-Teller splitting may also be essential to explain the experimental results in that region.

To summarize, we have calculated the KLM in the limit $S = \infty$ and $D = \infty$ on the Bethe lattice. Magnetic transition temperature is obtained exactly as a function of interaction strength and hole concentration. Comparison with the experimental data in $\text{La}_{1-x}\text{Sr}_x\text{MnO}_3$ is made. At $J/W \simeq 4$ and $W \simeq 1\text{eV}$, the model consistently explains the Néel temperature at $x = 0$ and Curie temperatures at $0.1 \lesssim x \lesssim 0.25$ in a quantitative way.

The author would like to thank Y. Tokura and T. Arima for fruitful discussions and comments. The numerical calculation is partially performed on the FACOM VPP500 at the Supercomputer Center, Inst. for Solid State Phys., Univ. of Tokyo.

References

- [1] C. Zener: Phys. Rev. **82** (1951) 403.
- [2] P. G. de Gennes: Phys. Rev. **118** (1960) 141.
- [3] Y. Tokura, A. Urushibara, Y. Moritomo, T. Arima, A. Asamitsu, G. Kido and N. Furukawa: J. Phys. Soc. Jpn. **63** (1994) 3931.
- [4] A. Urushibara, Y. Morimoto, T. Arima, A. Asamitsu, G. Kido and Y. Tokura: preprint.
- [5] N. Hamada: private communication.
- [6] K. Kubo and N. Ohata: J. Phys. Soc. Jpn. **33** (1972) 21.

- [7] A. J. Millis, P. B. Littlewood and B. I. Shraiman: preprint, SISSA:condmat/9501034.
- [8] N. Furukawa: J. Phys. Soc. Jpn. **63** (1994) 3214.
- [9] N. Furukawa: in *Proc. 17th Taniguchi International Conference*, edited by A. Fujimori and Y. Tokura (Springer Verlag, Berlin, 1995).
- [10] M. J. Rozenberg, G. Kotliar and X. Y. Zhang: Phys. Rev. **B49** (1994) 10181.
- [11] Y. Moritomo, A. Asamitsu and Y. Tokura: preprint.

Figure Captions

- Fig. 1:** Curie temperature T_c/W as a function of J/W .
- Fig. 2:** Curie temperature T_c at $J/W = 4$ and $J/W = \infty$ as a function of x . Experimental data in $\text{La}_{1-x}\text{Sr}_x\text{MnO}_3$ are from ref. 4. Temperature is scaled in the unit of Kelvin.
- Fig. 3:** Néel temperature at $x = 0$. The line in the figure is the result from $(J/W)^{-1}$ expansion.

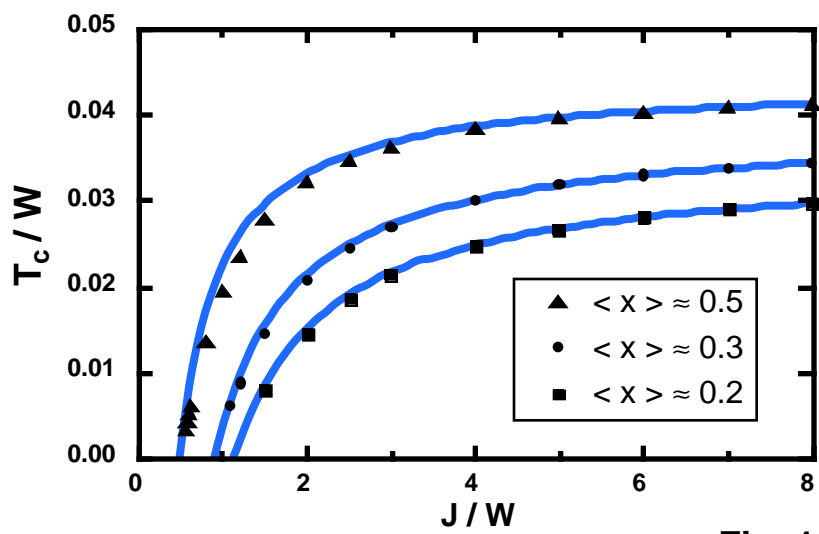


Fig. 1

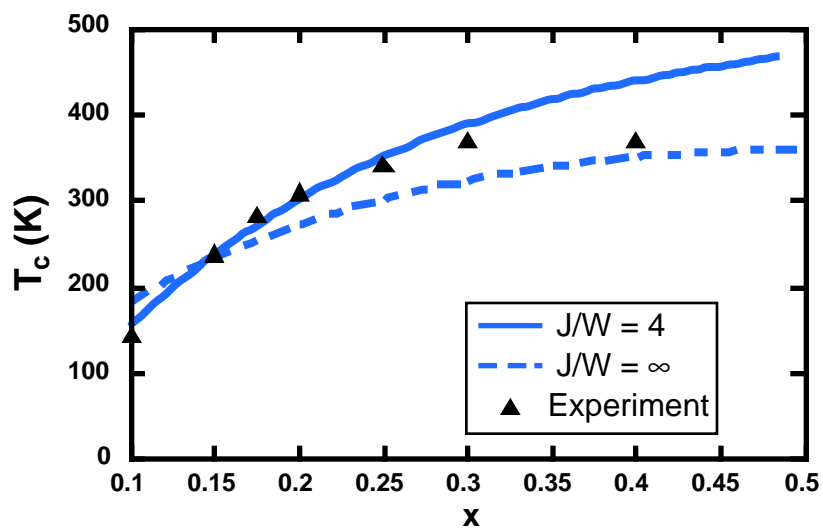


Fig. 2

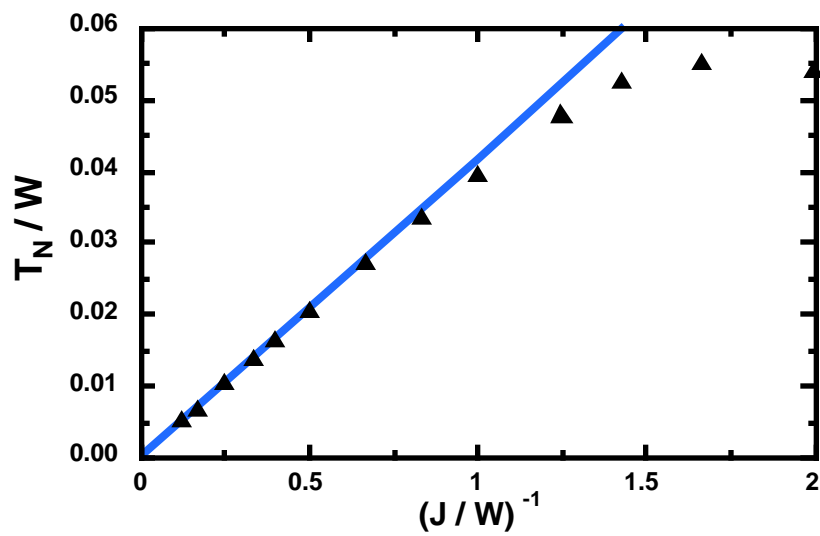


Fig. 3